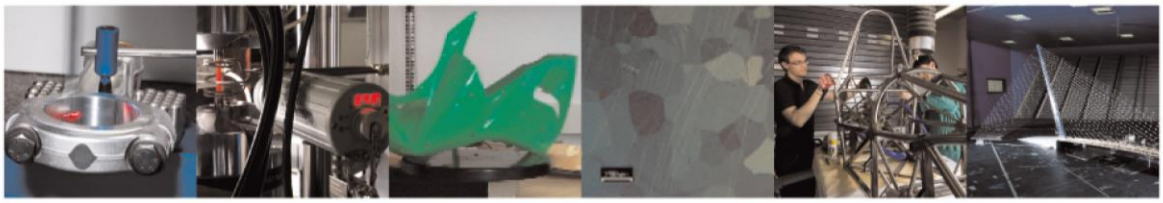

Impact of deep cores surface topography generated by micro milling on the demolding force in micro injection molding

Masato, Davide; Sorgato, Marco; Parenti, Paolo; Annoni, Massimiliano; Lucchetta, Giovanni

This is a post-peer-review, pre-copyedit version of an article published in JOURNAL OF MATERIALS PROCESSING TECHNOLOGY. The final authenticated version is available online at: http://dx.doi.org/10.1016/j.jmatprotec.2017.03.028

DIPARTIMENTO DI MECCANICA ■ POLITECNICO DI MILANO
via G. La Masa, 1 ■ 20156 Milano ■ EMAIL (PEC): pecmecc@cert.polimi.it
http://www.mecc.polimi.it
Rev. 0

Impact of deep cores surface topography generated by micro milling on the demolding force in micro injection molding

Davide Masato[a,†], *Marco Sorgato*[a], *Paolo Parenti*[b], *Massimiliano Annoni*[b], *Giovanni Lucchetta*[a]

[a] Department of Industrial Engineering, University of Padova, via Venezia 1, Padova, Italy

[b] Department of Mechanical Engineering, Politecnico di Milano, via La Masa 1, Milan, Italy

[†] corresponding author, davide.masato@dii.unipd.it

Abstract

In micro injection molding the quality of 3D complex parts is influenced by the efficiency of the ejection phase. During demolding, the forces taking place at the component-tool interface, due to adhesion and friction, need to be overcome preserving the integrity of the part. This issue is severe in the case of molds characterized by the presence of several deep cores, which are used to manufacture interconnecting through holes in multi-layer microfluidic devices. In this work, the impact of the micro milling cutting strategy on the demolding forces was investigated, using a critical cavity geometry, specifically designed to this purpose. The relation between mold micro manufacturing and the micro injection molding process was studied with the aim of optimizing the demolding phase. The topographies of micro-milled mold surfaces and the molded parts were characterized and different roughness profile parameters were taken in consideration. The results of in-line force acquisitions indicated that the effects of the micro milling strategy on the demolding force is markedly higher than those of micro injection molding process variables. Moreover, the experimental analysis indicated that a combination of worst surface finishing and low viscosity of the molding polymer can result in higher interface interlocking and thus in critical stresses applied to the part during the demolding phase.

Keywords: demolding, surface generation, micro injection molding, micro milling

Abbreviations

µIM	Micro injection molding
DoE	Design of Experiments
P_h	Packing pressure
t_c	Cooling time
V_{inj}	Injection speed
F_{peak}	Peak of the demolding force curve
F_{area}	Area subtended to the demolding force curve
COC	Cyclic olefin copolymer
PS	Polystyrene

1. Introduction

Lab-on-a-chip are devices integrating several complex laboratory functions on a single chip to achieve automated and high-throughput analysis. These devices find their main application in the biomedical industry, e.g. drug testing and DNA analysis, and their functionalities are allowed by the presence of several micro features on their surfaces. The research in this field aims at developing new devices allowing more complex analysis in a simple and economic way. Consequently, developing effective manufacturing process chains supporting their mass production becomes an issue (Attia et al., 2009). Indeed, Lucchetta et al. (2014) investigated the capabilities of the micro injection molding process in replication a micro-structured surface, highlighting the inherent limitations of the process.

In this context, micro injection molding (µIM) is a key enabling technology with the potential to mass-produce 3D complex parts at a low cost. However, the demand for increasing complexity, and the trend toward miniaturization, poses several technological issues. In particular, the filling and the ejection phases are critical steps in determining the efficiency of the process.

Lucchetta et al. (2016) observed that injection molding of micro parts is a challenging task because of the higher raise of cavity pressure that can prevent the complete replication of the mold geometry. On the other hand, Heckele and Schomburg (2003) suggested that part possessing dimensions or tolerances in the micrometric range make the ejection phase particularly critical. Thus, the understanding of process constraints for the production route is essential at both the design and manufacturing stages.

In µIM, the demolding phase is carried out through the application of ejection forces in some designed locations of the part, as indicated by Araújo and Pouzada (2002). Marson et al. (2011) observed that ejector pins can apply high local stresses to the part, causing possible distortion, stress marks and fractures.

Griffiths et al. (2010) described that ejector pins should overcome the local friction at the part-tool interface without damaging the final parts. Current solutions, based on intuition and experience, are not effective for complex micro parts and a unified systematic approach for solving demolding problems does not currently exist (Delaney et al., 2012). Thus, the development of systematic approaches to mold design, as well as process monitoring and optimization are required to improve the quality of micro-molded parts.

These issues are particularly critical in the case of multi-layer microfluidic devices, where the mold cavity has several features that counteract the shrinkage of the polymer melt. Indeed, the interconnections between the different layers are ensured by several arrays of through holes (Fig. 1) that are realized by a series of deep cores tools in the mold. Typical multi-layer microfluidic devices involve critical design conditions, which lead to manufacturing issues. In particular, the presence of small through holes is a common design solution that allows the exchange of small volumes of fluids between the device layers through small pipes. In order to reduce the device dimension, whilst maintain high complexity/functionality, the holes are commonly arranged in tight arrays. The combination of these design conditions makes μIM, and especially its ejection phase, particularly critical. In fact, Delaney and Kennedy (2010) described the development of demolding stresses during the μIM process, indicating how the normal force resulting from the polymer shrinkage affects the tangential force required during demolding and thus the efficiency of the demolding phase. Hence, the successful separation of the replicated part from the mold requires to develop a reliable micro manufacturing process chain.

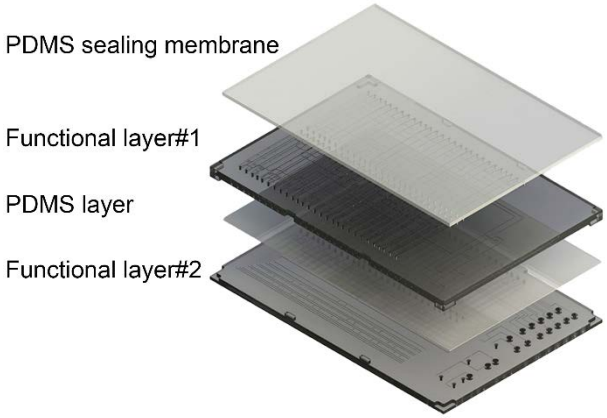

Fig.1: Example of multi-layer chip: 2 functional polymer layers - 2 PDMS sealing membranes.

The shrinking of the polymer part, constrained by the tool during the µIM process, causes an increase of the thermally-induced stress in the moldings, as described by Menges et al. (2001). The retaining forces that take place at the part-tool interface need to be overcome by a tangential force, generating a relative motion between the part and the tool. The successful manufacturing of plastic micro parts, characterized by high precision and good tolerances, requires to consider how the demolding force can be reduced (Marson et al., 2011). Hence, the factors influencing the demolding phase have to be understood and analyzed to avoid any detrimental effects on molded parts.

The polymer shrinkage in the µIM process can be controlled by appropriately selecting the controllable process parameters (Annichiarico and Alcock, 2014). In particular, a correlation exists between pressure during filling and packing phases and demolding parameters, as investigated by Griffiths et al. (2015). In their research, they showed that a proper combination of process parameters should be identified to achieve an optimal demolding behavior. Pontes and Pouzada (2006) noted that higher pressures reduce the differential shrinkage in the part, thus the diametric shrinkage and the consequent adhesion of the polymer to mold cores. However, Pontes and Pouzada (2004) reported that when the applied packing pressure was lower a smaller ejection force was observed, because of the larger through-thickness shrinkage that can cause smaller contact pressure at the part-tool interface. Moreover, the ejection forces are influenced by the process thermal boundary conditions. In particular,

the temperature of the part in the demolding phase determines the polymer elastic modulus and affects the part-tool interface friction (Pontes and Pouzada, 2004).

Pouzada et al. (2006) described the friction mechanism at the polymer-tool interface, indicating that it is also controlled by the mold temperature, which determines the interlocking between the polymer melt and the mold that is formed during the filling phase. In their work, they evaluated the coefficient of friction using a prototype apparatus showing that, due to replication, it can reach very large values (above 0.9).

Both the pressurized filling of the cavity and the shrinkage taking place during the part cooling, contribute to the surface interlocking, making the topography of the mold surface a fundamental parameter, as described by Ferreira et al. (2004).

Masato et al. (2016) analyzed the filling of a micro-structured surface by μIM, indicating that during the injection phase the polymer melt is driven into the mold cavity, and replicates the mold surface texture. Hence, the plastic part tends to stick over the cores surface after cooling, closely reproducing its surface finish. Therefore, the tribological conditions at the part-mold interface during the ejection phase are not only determined by the shrinkage-induced stresses, but also by the replication of the mold topography and the consequent mechanical interlocking. Moreover, Attia and Alcock (2009) studied the application of μIM processes to the replication of a micro-structured surface and they regarded the packing pressure as the main driving force that compels the polymer into micro cavities. Consequently, this process parameter should be considered as a possible cause of higher part-tool surface interlocking.

The interaction between the part and the tool at the beginning of the ejection phase determines the coefficient of friction between the two surfaces. The polymer part friction during the ejection phase can be interpreted considering a two-term non-interacting model that combines both adhesion and deformation contributions (Kim and Suh, 1991):

- adhesion is a surface effect, which derives from the physical attraction forces between metal atoms and polymer molecules close to the interfacial area (Wu, 1982);
- deformation is a bulk effect governed by the mechanical interlocking intensity between the replicating tool and the part, which produces two different kinds of friction mechanisms: ploughing of solid metal surface asperities over the soft polymer surface (Kim and Suh, 1993) and elastic deformation of polymer surface asperities (Suh et al., 1994).

The forces applied by the ejector pins, have to overcome the initial stiction by deforming the polymer side of the interface.

Micro injection molding tools are mainly produced by machining processes, such as micro milling (Fig. 2), characterized by an inherent surface roughness (Masuzawa, 2000). Parenti et al. (2017) investigated the generation of surface footprint in micro milling, analyzing the technological signature left by machining process on the generated mold surface.

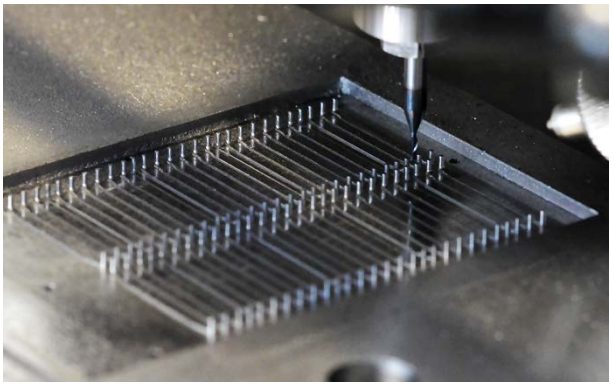

Fig.2: Micro milling of a lab-on-a-chip mold: 4 arrays of 28 pins - diameter 0.8 mm, height 2 mm.

The generation of the topography in micro-milled surfaces is particularly sensitive to tools, machine parameters and cutting strategy selection. In particular, the formation of burrs or smearing due to low uncut chip thicknesses can significantly influence the demolding phase (Huo, 2013).

Considering the effect of mold surface finishing on the ejection forces in conventional injection molding, Majewski and Hopkinson (2003) reported how they can be minimized reducing surface

roughness. In their work, they compared the effects of different surface finish, obtained with different processes, reporting improvements up to 50% of the total force required to demold the part. In fact, the coefficient of friction increases with roughness, as the expected influence of the surface asperities and the burrs mechanical effect (Schaller et al., 1999). Sasaki et al. (2000) used different polymers to investigate the effects of a wide range of surface finish (Ra from 0.016 to 0.689 μm) on the demolding force using a deep core tool geometry. Their results confirmed that ejection forces decrease with the mold roughness, but they found a limit beyond which the force increases. Correia et al. (2012) identified a lower limit for the average roughness Ra of the mold surface at 0.5 μm, below which the contribution of the adhesion force becomes relevant and cannot be neglected compared to the deformation. Hence, the optimization of the surface finish is fundamental in determining friction during the ejection phase, especially for manufacturing processes that produce intermittent smearing, such as micro milling (Delaney and Kennedy, 2010).

Yao and Kim (2004) discussed the importance of size effects of in miniaturization of injection-molded parts indicating that interfacial interactions are more relevant when processing at the micro scale, making the μIM process more sensitive to tool surface quality. Zhang et al. (2007) evaluated the relationship between the mold surface and the melt flow behavior in μIM, indicating that tool surface roughness affects the filling capabilities of the process by modifying the heat transfer at the part-tool interface. Consequently, the interaction occurring during the pressurized filling of the cavity can increase the adhesion between the polymer and the mold thus affecting the friction during the demolding phase (Berger et al., 2007). Even though surface roughness plays an important role during this phase (Giboz et al., 2007), the micro scale effects of mold topography produced by conventional machining processes has not yet been properly investigated.

In this work, the impact of the micro milling strategy on the reduction of the demolding force in micro injection molding was experimentally investigated. All the steps of the process chain were

accurately investigated in order to understand the effect of different mold surface textures on the optimization of the ejection phase.

In this study, the surface topography of the cores surfaces was generated with different micro milling strategies, considering the effect of different cutting parameters. The obtained mold inserts were then used to investigate the effect of µIM process parameters on the demolding force. A particular ejection system was realized to efficiently apply the demolding force around the deep cores and allowing the accurate force monitoring during the ejection phase. Both the frictional effects at the part-mold interface and the stresses produced in the part by the shrinkage during the injection molding cycle were analyzed.

Section 2 describes the part and the mold design, the applied micro milling strategies and the mold surfaces characterization. Section 3 discusses the µIM setup, focusing on material selection, process monitoring and experimental approach. The micro-milled mold surfaces characterization results are presented and discussed in Section 4. Section 5 analyzes and comments the µIM experiment results, considering the effects of the micro milling strategies on the ejection phase, the process variables and the molding material. Section 6 reports the topography characterization results of the molded parts and discusses the topography role on the demolding phase. Concluding, Section 7 reports the main results indicating how the whole process chain quality can be improved by controlling the interfacial interaction between the part and the tool, thus optimizing the ejection phase.

2. Mold design and manufacture

2.1 Part and mold design

The part considered in this study is a cylinder with a diameter of 6.8 mm and a thickness of 1.5 mm. The part is characterized by four through holes, having a diameter of 800 µm and no draft angles.

The part was specifically designed to study the effect of mold deep cores on the demolding force. In order to maximize the shrinkage of the polymer around the cores and to isolate the tribological phenomena at their interface, the lateral surface of the part was tapered of 18 degrees. Fig. 3 displays the geometry of the designed part.

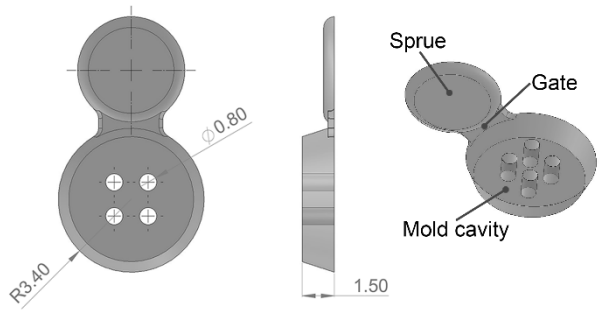

Fig.3: Design of the study part. All dimensions are expressed in millimeters.

A particular ejection system was realized by machining five cylindrical pins (diameter: 1 mm, aspect ratio: 3) on the top of a 6 mm diameter ejector rod, as displayed in Fig. 4. The pins served as small ejectors, which applied a distributed force around mold cores during the demolding phase.

The definition of the coupling tolerances between the ejector pins and their holes was critical, as it determined the final efficiency of the ejection system. Therefore, highly accurate micro milling strategies were implemented in the ejector rod and mold samples manufacture to satisfy the imposed micrometric tolerances.

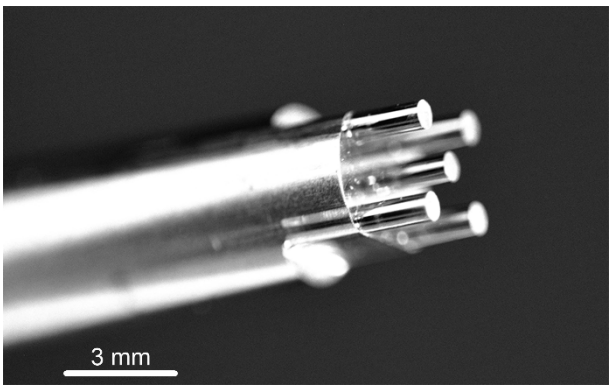

Fig.4: Main micro tooling components: ejector rod and micro-milled pins (diameter: 1 mm).

2.2 Mold surface generation

Three mold inserts and one ejector rod were produced by micro milling using an ultra-high precision machining center (Kern Evo) in a 3-axis configuration. Coated tungsten carbide end-mills were used for the machining operation. Fig. 5 displays the geometry of the cavity of one of the mold insert.

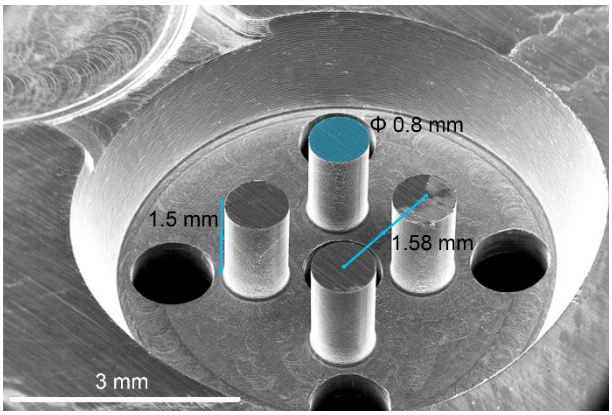

Fig.5: Main micro tooling components: mold cavity (SEM micrograph, magnification: 35x).

The three mold inserts were machined varying the milling strategies and the cutting parameters, based on state-of-the-art mold manufacturing strategies (Dhanorker et al., 2007) and on previous authors experience regarding high-aspect ratio micro milled features (Annoni et al., 2015). The design of the roughing and semi-finishing operations for the three mold samples was performed by using the computer-aided manufacturing (CAM) software CimatronE®.

Different micro milling cutting strategies and parameters were selected for finishing of the cores lateral surface, which is the interface between the mold and the plastic part. Considering the mold surface topography importance for the ejection phase, different mold textures were produced with the aim of minimizing the interaction between the steel and the polymer sliding over it, as it is required in presence of features constraining the shrinkage of the polymer melt.

All finishing operations were performed with 0.5 mm diameter round-end milling tools with a corner radius of 50 µm (Union Tool, HLRS 2005-005-020). A new tool was used for each mold insert to avoid tool wear effects.

Table 1 reports the micro milling cutting parameters that were varied for finishing the three mold inserts. Their selection is based on an experimental and theoretical investigations presented by Parenti et al. (2017).

Table 1: Micro milling strategies for the finishing operations of cores side.

Parameter	Insert 1	Insert 2	Insert 3
Strategy (Z axis)	axial	axial	helicoidal
Cutting Speed [m/min]	37.7	50.3	37.7
Feed [mm/tooth]	0.012	0.006	0.006
Axial Depth of Cut [mm]	0.5	0.5	0.012
Radial Depth of Cut [mm]	0.02	0.01	0.015

Different strategies were adopted among the mold samples, moving from a “constant step-down” approach (i.e. multiple vertical shifting of the tool along the z-axis), used for Insert 1 and Insert 2, to a “top-down helicoidal approach” (i.e. an helicoidal downward movement along the side of the mold core) adopted for Insert 3. From the surface texture point of view, this latter strategy allows to reduce the formation of geometric localized defects generated by the bending of the tool and the pin. On the other side, the surface re-machining caused by tool overlapping (unavoidable with the adopted 3-axis cutting configuration) demonstrated to generate lower average height amplitude but characterized by a more irregular surface pattern. The optimization of cores finishing also involved the selection of cutting speed, tool feed and depth of cuts (both axial and radial). In particular, axial depth of cuts adopted in Insert 1 and Insert 2 were constrained by the adopted step-down strategy, which requires the use of the maximum axial engagement of the end-mills (to avoid surface re-machining and tool overlapping). Insert 1 and Insert 2 were differentiated in terms of more demanding cutting parameters used for the

former sample, which generates bigger cutting forces and consequent higher tool-pin relative bending leading to bigger surface location errors. Indeed, feed per tooth used for Insert 2 and Insert 3 were fixed to a minimum value of 6 μm in order to reduce the impact of the uncut chip thickness effect. All of the samples were machined using a down milling cutting configuration since it is usually the most suitable approach for high aspect ratio features, as observed by Parenti et al. (2016).

The tight coupling tolerances between the ejector pins and the mold inserts were met by machining and measuring the ejector pins before manufacturing the mold inserts. Drilling operations of the holes for the ejector pins were then performed by correcting their nominal diameter on the base of the actual ejector pin diameters (measured with a CMM machine). The operations were conducted with two-flute ball-end milling tools (0.5 mm diameter) and helicoidal tool paths, generated by the CAM software, were adopted. To ensure the required accuracy roughing operations were followed by semi-finishing and finishing operations, using for this latter fresh end mills.

2.3 Mold surface characterization

The mold cavity geometry limited the optical accessibility to mold cores sides, thus hindering the possibility to directly characterize their surfaces using non-destructive techniques, such as non-contact optical metrology. Therefore, the characterization of the micro-milled surfaces was performed according to a first qualitative SEM observation and a subsequent topography analysis on the cut cores.

SEM (FEI, Quanta 400) analysis allowed the comparison of micro milling inherent machining marks and main topography defects of the different mold cores. Before SEM characterization, the mold inserts were cleaned using ultrasound with a cleaning solvent for 5 minutes. Then, the SEM micrographs of the inserts surfaces were obtained with an acceleration voltage of 20 kV, a working distance of about 18 mm and a secondary and back-scattered electron detector (Everhart-Thornley detector - ETD).

The manufactured inserts were then used for the µIM experiments and then inspected by means of destructive tests. Indeed, the mold inserts were cut after the molding tests to provide optical accessibility to the mold deep cores surfaces for their characterization. Direct surface measurements of the mold deep cores were then conducted using a 3D optical microscope with confocal/interferometer capacity (Mahr, MarSurf CWM 100) equipped with a 50x lens. The topographies of two pins for each mold insert were acquired along the whole length (scanning area: 0.386 x 1.200 mm), observing either the surface roughness and the presence of localized geometrical defects. The quantitative analysis on the acquired point clouds were conducted with MountainsMap® software. Five profiles (length: 1.2 mm) were extracted for each core and shape error was removed by using polynomial fitting already implemented in the software. Then, different roughness parameters were evaluated by applying an 80 µm Gaussian filter according to ISO 4287 and ISO 13565-2 standards.

3. Micro injection molding setup

3.1 Material and manufacturing system

A commercial polystyrene (TOTAL PS Crystal 1540) and a cyclic olefin copolymer (TOPAS, COC 5013L-10) were used in the µIM experiments. These materials were selected because of their high flowability and high transparency, which make them suitable for manufacturing lab-on-a-chip. Moreover, they are widely used for biomedical applications because of their good biocompatibility. Table 2 reports the main properties of these polymeric materials.

Table 2: Main properties of the investigated polymers.

Property	Units	Test Method	PS	COC
Density	g/cm^3	ISO 1183	1.04	1.02
MFI (200°C - 5 kg)	g/10min	ISO 1133	12	47
Tg	°C	ISO 6721	98.7	137.1

A rotational rheometer (TA Instruments, ARES) was used to determine polymers viscosity at temperature varying between 220 and 250 °C for polystyrene and between 240 to 300 °C for cyclic olefin. Comparing the flow curve for the two polymers, plotted using a Cross-WLF model calibrated on the experimental data, it is clear that COC has a lower viscosity than (Fig. 6). Hence, the replication capabilities of the μIM process are higher when using COC compared to PS.

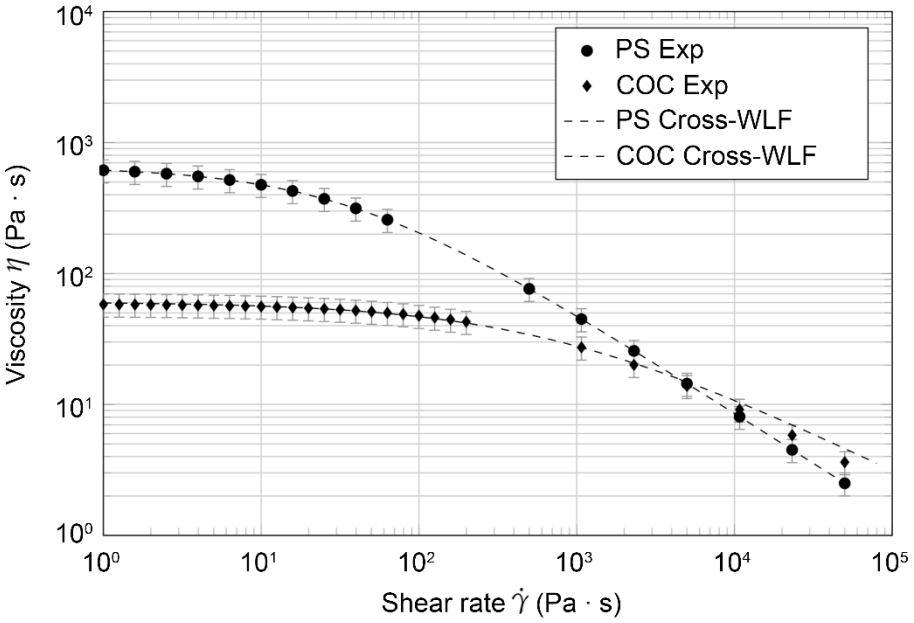

Fig.6: Experimental flow curve for the two polymers at μIM experimental melt temperature (i.e. 240 °C for PS and at 300 °C for COC).

A state-of-the-art μIM machine (Wittmann Battenfeld, MicroPower 15) with a maximum clamping force of 150 kN and a maximum injection speed of 750 mm/s was used for the experiments. The machine is characterized by an injection system divided into a 14 mm plasticizing screw and a 5 mm injection plunger.

The studied inserts produced using different micro milling cutting strategies were mounted onto the mold moving half. The mold heating system was implemented by using 4 electrical cartridges, two for each mold half, and two thermocouples, in order to guarantee a stable mold temperature.

3.2 Process monitoring

The force variations during the ejection stage were monitored by a Kistler 9223A piezoelectric force transducer (measuring range: 0-2500 N) positioned just behind the 6 mm diameter ejector rod (Fig. 7).

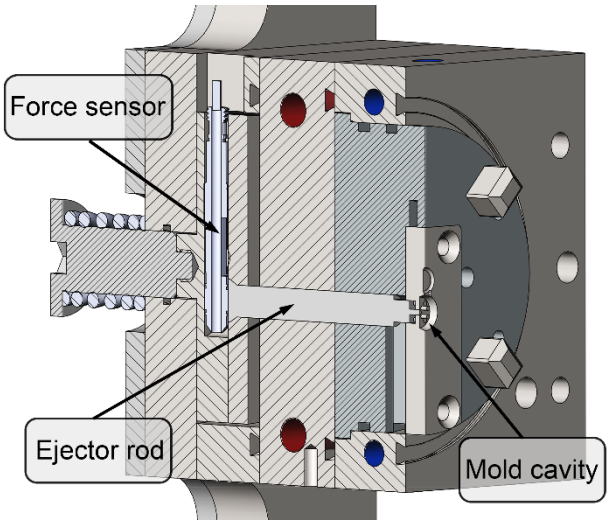

Fig.7: Mold assembly - details of the moving half.

During the part demolding, the transducer was subjected to a mechanical load producing a piezoelectric charge signal. This signal was converted into an output voltage using a Kistler Type 5039A charge amplifier and acquired by a National Instruments NI9205 16 bit analog input module. The sensor output signal was then downloaded onto a PC by a National Instrument NI cDAQ-9172 data acquisition unit and the measured values were analyzed using the National Instruments Labview 2013® software. Ten samples were acquired at a rate of 60 kHz, i.e. with a time step of 0.2 ms, in order to guarantee the collection of the whole demolding force profile, without any data loss.

3.2.1 Dry cycling

The assembly and the functionality of the mold were initially evaluated with several dry cycles of the µIM machine clamping and ejection units. Indeed, the tight fit between the holes in the mold insert and the ejector pins, machined on the top of the ejector rod, needed to reach a stable behavior. The ejector was cycled 200 times (ejector stroke: 0.8 mm; ejection speed: 10 mm/s), allowing the evaluation of the functionality and robustness of the demolding force acquisition setup. The cycles were performed at a mold temperature of 50 °C that was the same value set in the following µIM experiments.

The dry cycle trend analysis indicated how the ejection force reaches a stable value after 200 cycles, as shown in Fig. 8. Moreover, the stabilized value of the dry demolding force was smaller than 1 N for all the produced mold inserts. Consequently, the dry force was not considered when comparing tests made with different mold inserts in the following analysis.

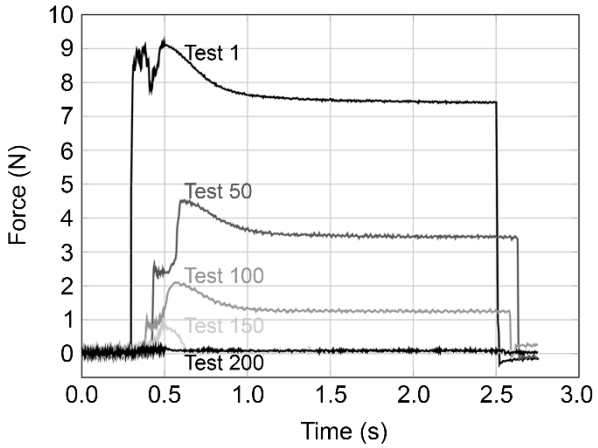

Fig.8: Stabilization behavior of the dry ejection force over cycles for Sample 1.

3.3 Experimental approach

3.3.1 Screening phase

The combined effect on the ejection force of polymer shrinkage and surface finish was studied in relation with the main µIM process parameters by applying a design of experiments (DoE) approach.

To characterize the effects of mold surface finish and µIM parameters on the demolding force variation (screening phase), a four-factor full factorial design was carried out, using PS as molding material. In addition to the micro milling strategy, the other process variables selected for the analysis were the packing pressure P_h, the cooling time t_c and the injection speed V_{inj}. The range values for each factor are reported in Table 3. During the µIM tests, the following parameters were fixed:

- mold temperature: 50 °C;
- melt temperature: 240 °C;
- metering size: 1.2 mm;
- packing time: 2 s;
- clamping force: 120 kN.

Table 3: Process parameters settings for the screening DoE plan.

Factor	Low level	Medium level	High level
Insert	1	2	3
P_h [bar]	40	-	80
t_c [s]	2	-	10
V_{inj} [mm/s]	50	-	300

The range values for the DoE screening plan and the fixed parameters values were defined considering the literature, recommendations of the material supplier (max. nozzle melt temperature 210-240 °C) and technological limitations of the available experimental setup.

3.3.2 Optimization

Considering the results of the screening phase (sections 5.1, 5.2), the ejection phase optimization was then carried forward by investigating the effect of a different polymer. In particular, the COC was introduced in the µIM experiments.

To investigate the effect of the polymer, a two-factor full factorial plan was designed including the micro milling strategy as the only other parameter (Table 4). According to the results of the screening phase, the μIM process parameters were fixed to the following values:

- injection speed: 300 mm/s;
- packing pressure: 40 bar;
- cooling time: 10 s.

The other fixed parameters were held to the screening phase values.

Table 4: Process parameters settings for the optimization plan.

Factor	Low level	Medium level	High level
Insert	1	2	3
Material	PS	-	COC

3.3.3 Response variable

The understanding of the ejection force reduction effects on process quality needs to consider all the mechanical loads applied to the plastic part during the demolding phase. For this reason, the response variables selected for both the DoE campaigns were the demolding force peak F_{peak} and the subtended area F_{area}, as shown in Fig. 9. Indeed, the acquired force peak represents the maximum load stressing the molded part, while the curve subtended area stands for the demolding work, under the hypothesis of constant speed of the ejectors.

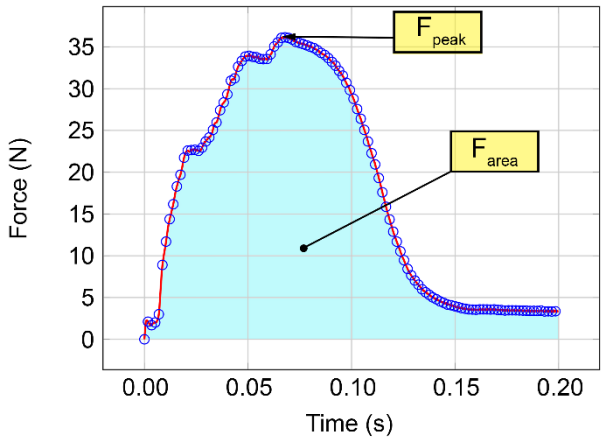

Fig.9: Response variables for the statistical analysis of the experimental data.

To guarantee the µIM process and the online force monitoring setup stability, 10 molding cycles were carried out before the first demolding force acquisition. Then, 5 acquisitions were collected, one every 5 cycles, for each molding condition. The acquired data were then aligned to the beginning of the ejection phase and overlapped to evaluate their repeatability (Fig. 10). The response variables were then calculated and collected for each DoE combination using Matlab.

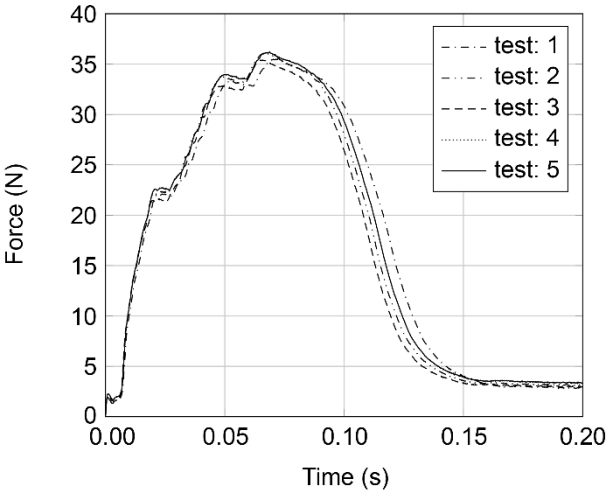

Fig.10: Example of demolding force in-line acquisitions of DoE repetitions - std. dev. F_{peak}: 0.38 N, F_{area}: 0.75 N·s.

3.4 Characterization of the molded parts

The through holes topographies of the molded parts were evaluated in order to improve the understanding of the relation between the mold surface topography and the micro manufacturing process. The µIM molded parts were micro-milled (Kugler, Micromaster 5X) in order to make the 800 µm holes accessible and then inspected using a SEM (FEI, Quanta 400) and a 3D optical profiler (Sensofar, Plu Neox) operating in confocal mode with a 20x objective.

In order to evaluate the µIM molded parts roughness, the topography of two holes for each replication and each run of the optimization plan was acquired in a projected area of 0.4 x 1.5 mm. Topographies were analyzed using the MountainsMap® software, to evaluate different profile roughness parameters. Three profiles where extracted for each measurement (length: 1.5 mm), the shape error was corrected and the selected roughness parameters were evaluated applying a 80 µm gaussian filter, according to ISO 4287 and ISO 13565-2.

Summarizing, for each treatment and each of the five replicas of the optimization plan, the surface topography of two through holes was acquired. Then for each acquisition three profiles were extracted and the roughness parameters were evaluated; for a total of 30 profiles evaluated for each experimental condition.

4. Mold surface analysis results

4.1 Mold topography characterization

The mold inserts surface topography characterization, initially performed by means of SEM, showed some differences in terms of surface finish moving from Insert 1 to Insert 2 and Insert 3, as visible in Fig. 11 (a), (b), (c). This fact confirms the expected micro milling strategy and cutting parameters effect on the mold surface topography.

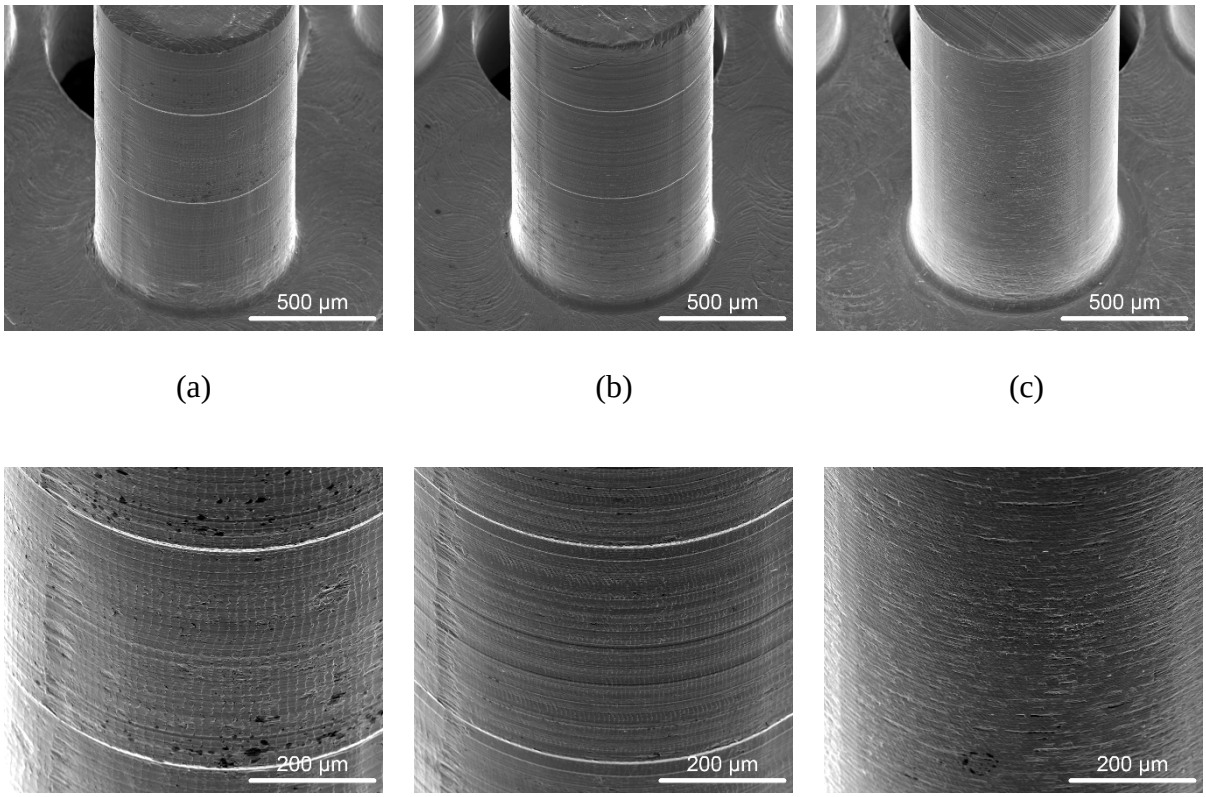

Fig.11: SEM micrographs of the micro-milled mold inserts at different magnifications. Insert 1 at (a) 200x and (d) 500x; Insert 2 at (b) 200x and (e) 500x; Insert 3 at (c) 200x and (f) 500x.

All the manufactured mold inserts are characterized by the presence of an inherent surface texture, typical of micro-milled surfaces. However, the topographies of Insert 1 and 2 are characterized by more evident feed marks with some minor smearing effects, due to the milling tool ploughing over the surface (Fig. 12).

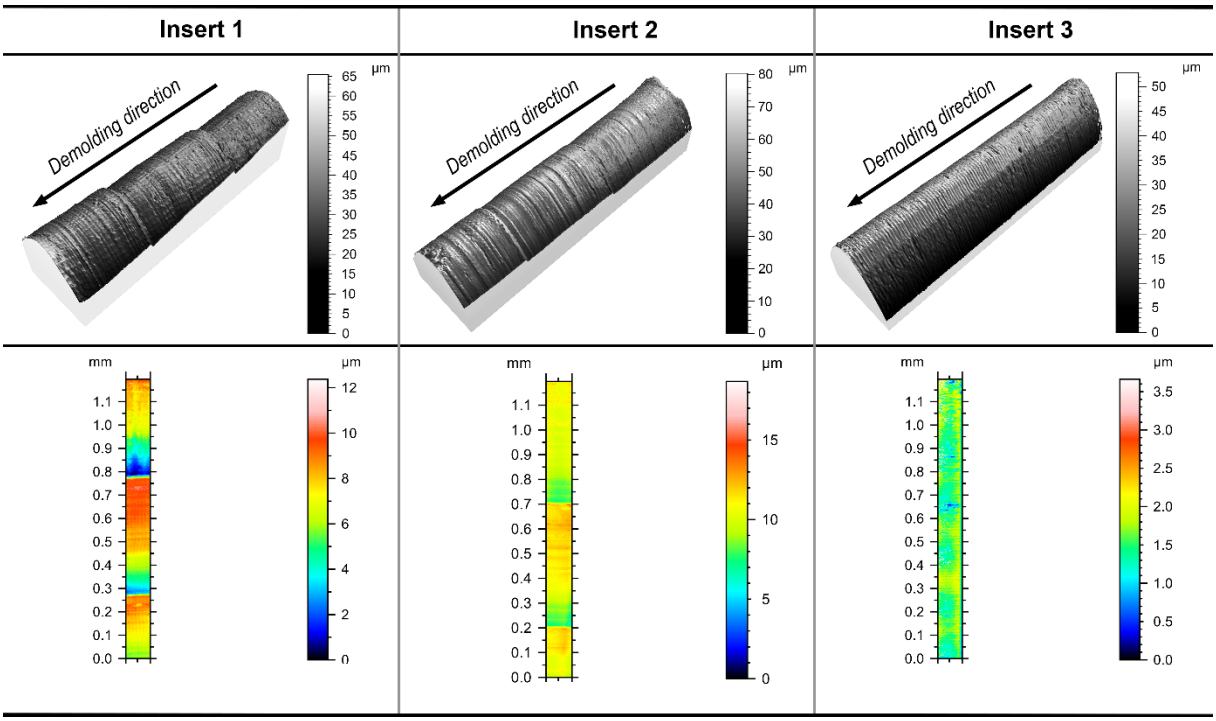

Fig.12: 3D and 2D views of the three mold insert topographies.

On the contrary, the ploughing and smearing action dominates Insert 3 due to its helicoidal tool path with small axial depth of cut. In this case, the tool repeatedly passes over the already machined surface producing a smooth and smeared finish.

The micro milling process generated on the mold inserts also localized geometrical defects, as clearly visible in Fig.11. On one side, the entire inserts showed four regularly spaced marks oriented in the vertical direction (with an angular shift of about 90 degrees). Their presence is compatibly related with machine axes inversion errors, caused by the circular tool trajectory on the X-Y plane. They showed relatively large height amplitude with respect to surface roughness. Despite that, their limited width (around 50 µm) and their vertical orientation make them assuming a minor role on the demolding forces generated by the molds.

Moreover, the strategy adopted for the movement of the tool in the vertical direction affected the formation of localized geometrical defects oriented in circumferential direction. Indeed, the presence of two micrometric circumferential steps, oriented oppositely to the demolding direction, was observed

for mold Insert 1 and Insert 2 (Fig. 11 (d), (e)). These vertical discontinuities constitutes micro milling-derived form error of the deep cores and represent possible undercuts for the ejection phase of the µIM process. The average height of these defects, evaluated on the topographies acquired on the manufactured mold inserts, was 6.8 µm for Insert 1 and 3.3 µm for Insert 2. The presence of these steps was not observed in case of Insert 3, where a helicoidal tool path was applied (Fig. 11 (f)).

4.2 Roughness evaluation

Table 5 reports the roughness characterization results, indicating an evident effect of the micro milling strategy on mold surface roughness (ISO 4287).

Table 5: Average values and standard deviations of profile roughness parameters evaluated according to ISO 4287 and ISO 13565-2.

		ISO 4287				ISO 13565-2		
Insert		Rz [µm]	Ra [µm]	Rq [µm]	Rku	Rk [µm]	Rpk [µm]	Rvk [µm]
1	Avg. Val.	4.09	0.34	0.57	6.97	0.52	1.29	1.24
	Std. Dev.	0.61	0.05	0.06	0.41	0.12	0.13	0.11
2	Avg. Val.	2.17	0.21	0.30	5.05	0.53	0.46	0.66
	Std. Dev.	0.37	0.02	0.03	0.78	0.06	0.04	0.09
3	Avg. Val.	1.30	0.13	0.18	5.81	0.35	0.15	0.32
	Std. Dev.	0.35	0.03	0.04	1.89	0.06	0.04	0.11

Micro milling cutting parameters affect both the presence of protruding peaks in the profile (Rz) and the overall roughness of the mold surface (Ra, Rq). In particular, the average value of Ra reduces by 39% by changing the cutting parameters from Insert 1 to Insert 2, and by 62% from Insert 1 to Insert 3.

The kurtosis parameter (Rku) was considered to measure the sharpness of the height distribution, which can potentially affect the friction between the mold surface and the polymer part during the ejection phase. As shown in Fig. 13(a), the Rku evaluated for the three mold samples is not

significantly different, indicating that the micro milling process produced surfaces characterized by similar morphologies under this point of view.

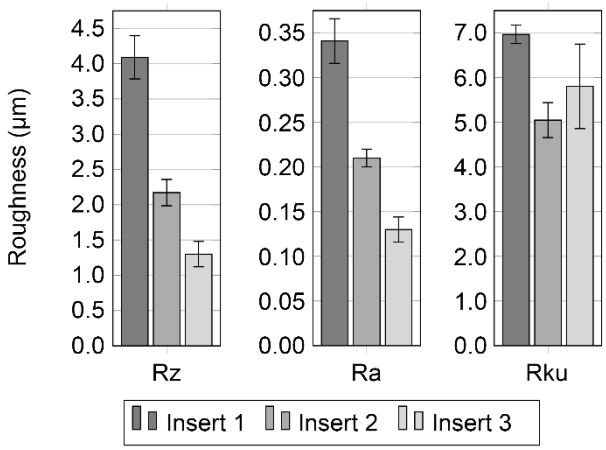

(a)

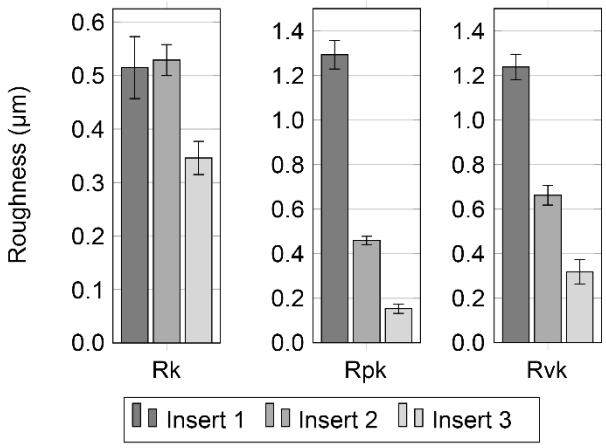

(b)

Fig.13: Histograms of roughness parameters for (a) ISO 4287 and (b) ISO 13565-2.

However, amplitude parameters do not provide information about the shape, slope and size of the asperities or about the spatial frequencies of their occurrence (Dong et al., 1994), which can be important in determining the performance of the µIM ejection phase. Hence, in order to improve the understanding of the interface interaction between the mold surface and the replicating polymer, the Abbott-Firestone curves were evaluated (Tao Zhang et al., 2006). According to ISO 13565-2, this curve allows the

determination of the Rk parameters from the linear representation of the material ratio curve that describes the increase of the material portion of the surface with increasing the roughness profile depth ISO 13565-2. The curve provides information about the material and void volumes characterizing the surface topography, thus being important to study the potential replication behavior of different μIM mold surfaces (Lucchetta et al., 2011).

Table 5 reports the Rk parameters values for the three micro-milled mold surfaces. The Rk values are about the same for Insert 1 and 2, while they are significantly different for Insert 3, as shown in Fig. 13(b). The values of Rpk and Rvk are significantly different for the three micro-milled inserts. In particular, they reduce from Insert 1 to Insert 2 to Insert 3.

High values of Rvk can negatively affect the ejection forces because of the higher void volumes in the mold surface, which can be replicated by the polymer that fills them causing higher interfacial interactions. Similarly, high values of Rpk can lead to increased friction between the mold and the part, because of the markedly higher presence of protruding peaks that causes higher demolding stresses.

5. Micro injection molding results

The developed experimental plans were analyzed to identify the significant factors on the demolding force. In order to perform a univariate analysis of variance (ANOVA), a general linear model was fitted to the experimental data. The statistical significance of the factors included in the model was evaluated comparing the p-values with a threshold value of 0.05. The factors having a p-value lower than 0.05 can be considered statistically significant on the selected response.

The results reported in Table 6, indicate that all the main effects significantly affect both the demolding force peak F_{peak} and subtended area F_{area}. Moreover, some first-order interactions included

in the model are statistically significant. The detailed analysis of the selected variables effects on the demolding phase is discussed in the following Section 5.1 and Section 5.2.

Table 6: Anova table for the screening experiments designed in Table 3.

	p-value	
	F_{peak}	F_{area}
Insert	0.000	0.000
P_h	0.000	0.000
t_c	0.000	0.001
V_{inj}	0.000	0.007
Insert·P_h	0.000	0.000
Insert·t_c	0.000	0.000
Insert·V_{inj}	0.000	0.000
P_h·t_c	0.004	0.317
P_h·V_{inj}	0.000	0.000
t_c·V_{inj}	0.046	0.000

5.1 Effect of the micro milling strategy

The effect of the micro milling parameters on the ejection force is significant for both F_{peak} and F_{area} (p-value: 0.000). The effect of improving the cores surface finish by changing the micro milling parameters from Insert 1 to Insert 2 and from Insert 1 to Insert 3 is to reduce F_{peak} by respectively 28.2% and 51.1% (Fig. 14), and the Farea by respectively 0.3% and 31.5% (Fig. 15).

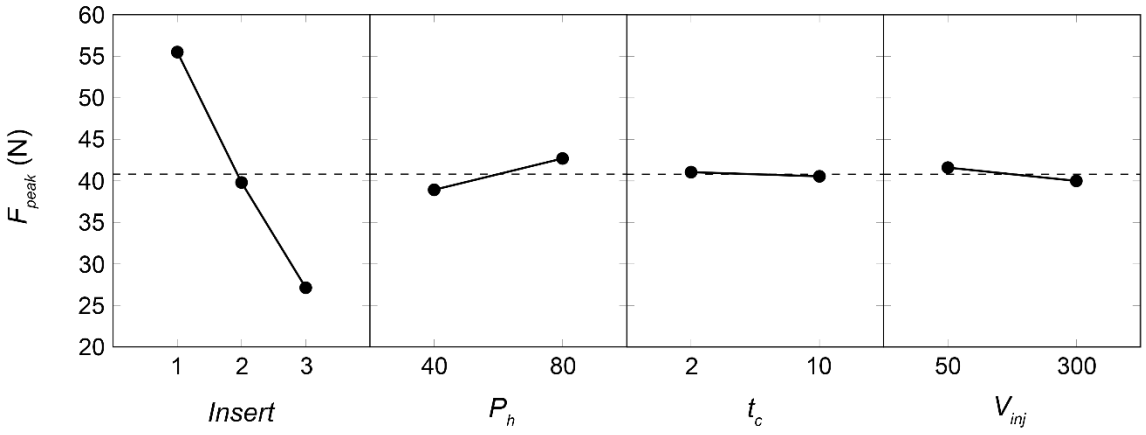

Fig.14: Main effect plots for the demolding peak force F_{peak} (screening plan).

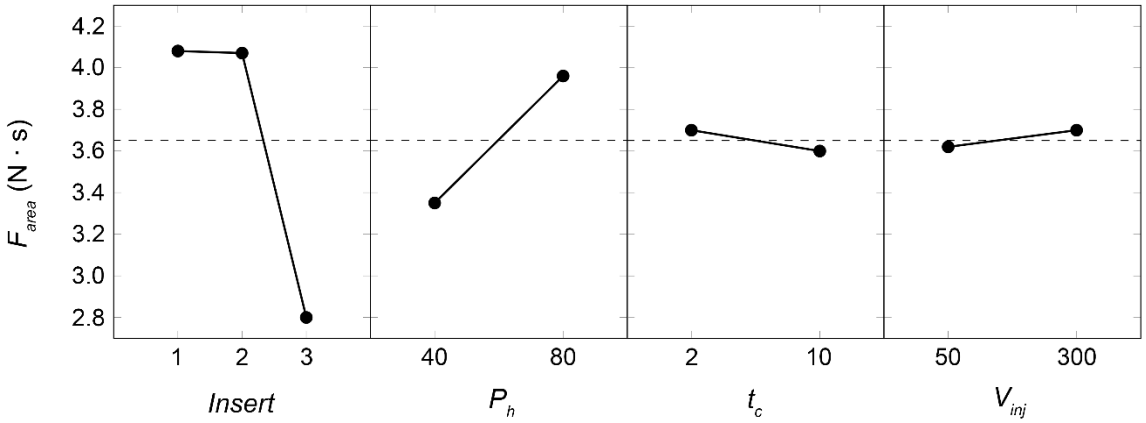

Fig.15: Main effect plots for the demolding work F_{area} (screening plan).

Comparing the effect of the three mold inserts, it was observed that the shape of the curves is the same, as shown in Fig. 16. However, it is clear that the mold surface topography markedly affects the values of the force applied to the molded parts during the demolding phase. The maximum overall ejection force was acquired when using mold Insert 1, indicating that the plastic was subjected to the highest stress during the ejection phase with this mold topography.

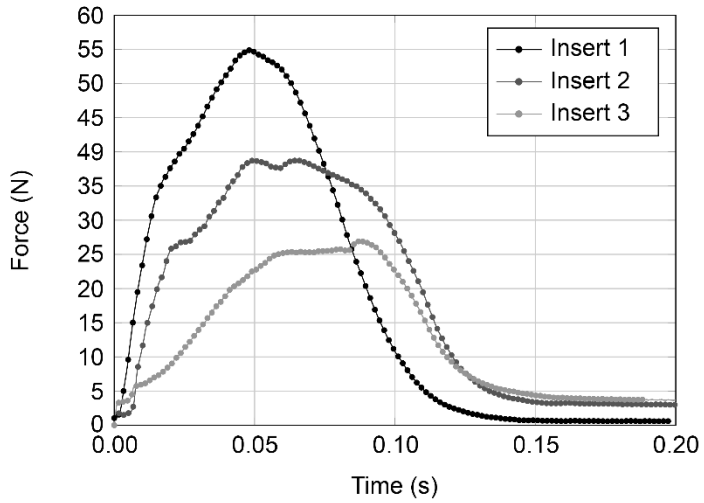

Fig.16: Effect of the micro milling strategy on the demolding force curves - max. standard deviation: 0.5 N.

The higher demolding forces observed for Insert 1, which was produced with a combination of higher micro milling cutting parameters (i.e. feed and depths of cut), are explained by its worst surface

finish. This fact is confirmed by the mold surface characterization (Section 4), which showed that Insert 1 presents the larger asperities compared to other micro-milled mold inserts.

The higher the mold surface roughness, the higher the resistance at the part-tool interface. In fact, when filling the cavity, the polymer melt can replicate the surface topography of the mold and, as a consequence, produce interlocking between the two surfaces. Then, the force required to initiate the solidified polymer sliding over the mold steel surface is higher and so is the demolding force peak. By improving the mold surface roughness, F_{peak} gets lower as also the mechanical effect of surface asperities is smaller. During the ejection, the sliding of the two solid surfaces is characterized by localized ploughing and deformation mechanisms that increase in case of worst mold surface finish.

The demolding force reduction is consistent with the surface roughness reductions quantified on the mold cores. The amplitude parameters able to represent the micro milling strategy effect on F_{peak} are Rz (-47% from Insert 1 to Insert 2, -68% from Insert 1 to Insert 3), Ra (-39%, -62%) and Rq (-47%, -68%). Moreover, Rpk (-65%, -88%) and Rvk (-47%, -74%) decrease as F_{peak} when changing the micro milling parameters.

The main effect of the micro milling strategy on F_{area}, displayed in Fig. 15, is more or less insignificant moving from Insert 1 to Insert 2. On the contrary, the reduction is markedly evident moving from Insert 2 to Insert 3. This fact is explained by the presence of two circumferential undercuts, responsible for higher F_{area} in mold Insert 1 and Insert 2. The absence of this geometrical defect in Insert 3, thanks to the micro manufacturing strategy improvement, led to a significantly lower demolding energy.

The F_{peak} values are more sensitive to mold surface finish improvements because of the large part-tool interlocking effect on the static friction, which directly influences the maximum value of the load applied to the part. Indeed, the energy absorbed during the ejection phase F_{area} depends on the dynamic

friction between the two sliding surfaces, which is less affected by a topographical defects reduction (i.e. cores surface finish improvement).

5.2 Effect of μIM process parameters

Considering the ANOVA results, it is clear that the thermal shrinkage of the polymer around deep cores is an important factor affecting the stress generated during the demolding phase. The contact pressure generating during the μIM cycle and determining the ejection friction, is produced by the effect of process parameters on the polymer thermal shrinkage, such as the packing pressure.

The main effect of increasing the packing pressure from 40 to 80 bar is to increase F_{peak} by 10% and F_{area} by 18% (Fig. 14, 15). In fact, high values of P_h affect the replication of deep cores topography, determining a higher mechanical interlocking between the part and the mold. This is supported also by the significance of the first order interaction between the Insert and the P_h (p-value: 0.000), which showed larger effect of the packing pressure for worst surface finish. Thus, the higher adhesion at the interface, resulting from a higher replication, prevails over the expected reduction of the contact pressure at the part-mold interface that is caused by a lower diametric shrinkage. Moreover, as suggested by Pontes and Pouzada (2004), at low values of the packing pressure the part and the mold surfaces are likely to separate, causing a reduction of the heat transfer and keeping the polymer at a higher temperature during the demolding phase.

As shown in Fig. 14 and Fig. 15, the main effects of the cooling time and injection speed are less important than the other factors considered in the analysis, indicating that their effect on both the topography replication and the contact pressure was not significantly improving the demolding phase.

5.3 Effect of molding polymer

Selecting a different molding polymer resulted statistically significant according to the optimization plan ANOVA (p-value: 0.000) reported in Table 7. In particular, using COC instead of PS produced an average increase of the demolding force peak and work by 69% and 104% (Table 8).

Table 7: Anova table for the optimization experiments designed in Table 4.

	p-value	
	F_{peak}	F_{area}
Insert	0.000	0.000
Material	0.000	0.000
Insert·Material	0.000	0.000

Table 8: Experimental results of the optimization plan.

		F_{peak} [N]		F_{area} [N·s]	
Insert	Polymer	Avg. Val.	Std. Dev.	Avg. Val.	Std. Dev.
1	PS	49.9	0.3	3.6	0.1
2	PS	35.7	0.4	3.5	0.1
3	PS	25.8	0.1	2.6	0.1
1	COC	95.2	0.6	9.5	0.3
2	COC	60.3	0.5	6.4	0.1
3	COC	33.1	0.5	3.7	0.1

The effect of the molding material on the ejection phase stress is related to a combination of higher shrinkage properties and lower viscosity, at the selected melt temperature. In particular, the COC was reported to be more prone to higher interactions at the part-tool interface during the µIM process (Sorgato et al., 2016).

The analysis of variance indicated that the influence of the first order interaction between the mold insert and the polymer is important for a complete understanding of the effect of the micro milling strategy on the ejection phase. In particular, the better the mold surface finish the smaller the difference between the force values acquired for the two polymers, as shown in Fig. 17.

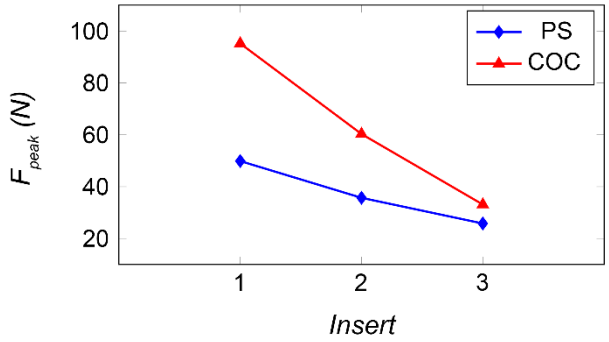

(a)

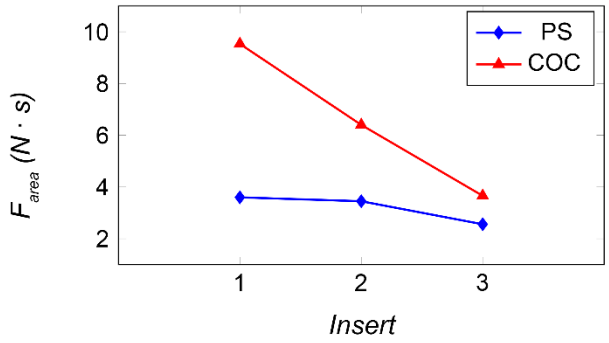

(b)

Fig.17: Interaction plot for the optimization plan. (a) demolding force peak; (b) demolding force area.

A combination of worst mold surface finish (i.e. Insert 1) and low viscosity of the polymer (i.e. COC) resulted in higher demolding friction, because of the markedly higher interlocking at the tool-part interface. In fact, COC gives a better replication of the mold surface topography, thus causing a higher interfacial interaction. On the contrary, improving the mold surface finish attenuated the interlocking and consequently the influence of the polymer.

6. Molded parts roughness evaluation

The effects of different polymers on the tribological conditions during the ejection phase are due to the different mold surface topography replication that they obtained. In particular, the worst the surface finish the larger the volume that can be filled by the polymer during the injection phase.

Specifically, the average depth of the profile valleys projecting through the roughness core profile Rvk increased from Insert 1 to Insert 2 to Insert 3.

Table 9 reports the roughness parameters evaluated for each run of the optimization plan on the inner surface of the through holes in the molded parts. The values of Rz, Ra, Rq and Rk indicate that a clear effect of the mold surface topography exists on the molded parts roughness. Indeed, the higher the mold replication obtained during the injection phase, the rougher the part surface after the ejection phase. The Ra values observed in the molded parts decrease from Insert 1 to Insert 2 and from Insert 1 to Insert 3 by 23% and 50%, respectively. The same trend was observed for Rz (23%, 52%), Rq (18%, 48%) and Rk (35%, 52%), as shown in Fig. 18.

Table 9: Molded parts roughness (optimization plan).

Insert	Material		Rz [µm]	Ra [µm]	Rq [µm]	Rku	Rk [µm]
1	PS	Avg. Val.	2.18	0.29	0.38	3.94	0.91
		Std. Dev.	0.28	0.03	0.04	1.07	0.13
2	PS	Avg. Val.	1.66	0.22	0.29	3.85	0.62
		Std. Dev.	0.27	0.03	0.04	0.43	0.17
3	PS	Avg. Val.	1.03	0.14	0.18	3.31	0.44
		Std. Dev.	0.13	0.02	0.02	0.45	0.08
1	COC	Avg. Val.	2.68	0.35	0.42	4.07	1.17
		Std. Dev.	0.12	0.03	0.05	0.55	0.06
2	COC	Avg. Val.	2.10	0.27	0.36	3.99	0.73
		Std. Dev.	0.38	0.04	0.06	0.67	0.13
3	COC	Avg. Val.	1.30	0.18	0.23	3.66	0.55
		Std. Dev.	0.21	0.02	0.03	0.94	0.10

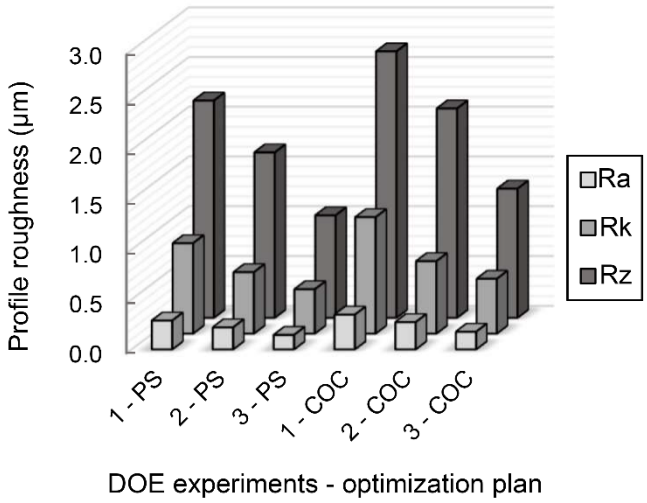

Fig.18: Roughness amplitude parameters evaluated on the plastic parts.

Rku values, instead, do not show significant variations, indicating that all the parts are characterized by the same height distribution sharpness after demolding. It seems that, regardless of the mold surface topography and molding material, the mold surface asperities produced the same surface morphology.

Considering all the profile parameters evaluated on parts molded with different polymers, it was found that the roughness was smaller on PS than on COC, indicating that the replication of mold surface topography is markedly higher with COC. The effect of micro milling strategies and molding polymers on the demolding phase was confirmed by observing the inner surface of molded parts with SEM, as shown in the micrographs reported in Fig. 19. In particular, it is clear that the part surface is characterized by a smoother topography with less asperities for inserts with improved surface finish. Moreover, the higher replication obtained with COC was observed by comparing parts made with the two different polymers. This fact confirms the higher interlocking and the consequent higher friction between part and tool in case of COC.

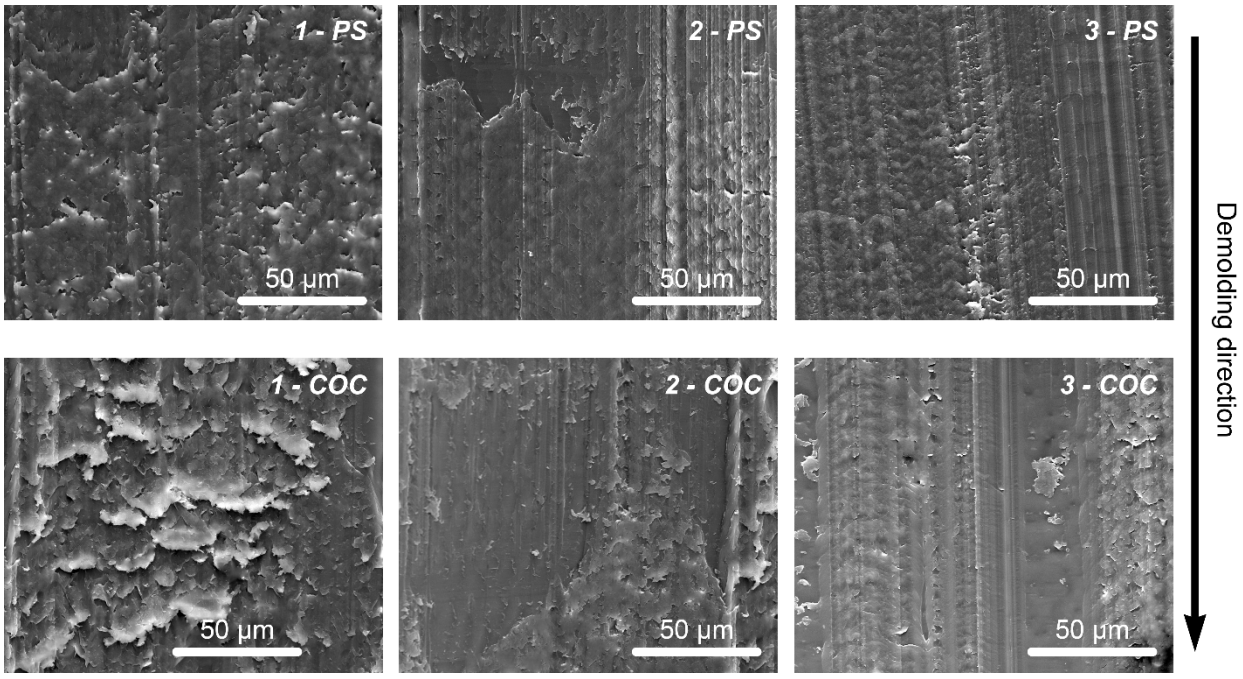

Fig.19: SEM micrographs of the molded parts topographies - magnification: 2000x.

7. Conclusions

The main objective of this study was the investigation of the impact of different micro milling cutting strategies on the µIM demolding phase. Three different mold surfaces were manufactured using an ultra-high precision machining center and their topographies were evaluated considering different profile roughness parameters and the presence of localized geometrical defects. The cavity geometry was designed to study the tribological conditions at the interface between the polymer and the tool deep cores. The demolding phase was optimized by means of design of experiments, considering the combined effect of polymer replication onto deep cores and surface finish, in relation with the main µIM process parameters.

The results of the mold topographies characterization indicated that improved milling parameters and strategy led to a lower profile roughness (i.e. less feed marks and asperities). In particular, changing the micro milling strategy from Insert 1 to Insert 2 and from Insert 1 to Insert 3 resulted in decreasing Ra by 39% and 62%, respectively. The inserts Abbott-Firestone curve was evaluated,

observing how Rpk and Rvk decreased when improving the micro milling strategy, thus affecting the presence of protruding peaks and void volumes in the topographies and consequently determining different tribological conditions at the interface during part demolding.

The analysis of the µIM demolding force in-line acquisitions showed that the demolding force peak reduced, compared to Insert 1, by 28.2% for Insert 2 and by 51.1% for Insert 3. These values are consistent with the surface roughness reductions quantified on the mold cores, thus indicating that controlling mold texture generation is a key factor. The demolding force work reduction was smaller (0.3% and 31.5% respectively) because of the lower effect of the interlocking at the part-tool interface on the dynamic friction.

The effect of µIM process parameters was considerably smaller compared to that of mold surface finish. In particular, increasing the packing pressure resulted in higher demolding stress due to the higher replication and consequently higher mechanical interlocking at the part-mold interface. On the contrary, the effects of cooling time and injection speed were less significant in improving the demolding phase.

The molding polymer affected the ejection phase by modifying the interface interactions between the part and the mold. In particular, a combination of worst surface finishing (Insert 1) and low viscosity (COC) resulted in higher replication of the cores surface topography and thus in higher demolding forces. This replication-related effect was investigated by evaluating the molded parts through holes inner surface roughness. Results indicated that main roughness parameters (Rz, Ra, Rq, Rk) were smaller for PS parts compared to COC parts, pointing out that less polymer deformation and ploughing occurs in the former case. Moreover, the molding polymer was observed to interact with the different micro milling strategy selection. In fact, the better the surface finish, the smaller the possibility for the melt polymer to replicate the mold topography, thus producing smaller interface interlocking and consequently less demolding stresses.

Funding

This research did not receive any specific grant from funding agencies in the public, commercial, or not-for-profit sectors.

References

Annicchiarico, D., Alcock, J. R., 2014. Review of factors that affect shrinkage of molded part in injection molding. Materials and Manufacturing Processes, 29(6), 662-682.

Annoni, M., Rebaioli, L., Semeraro, Q., 2015. Thin wall geometrical quality improvement in micromilling. The International Journal of Advanced Manufacturing Technology, 79(5-8), 881-895.

Araújo, B. J., Pouzada, A. S., 2002. Design of ejection systems for injection moulds. O Molde, 54, 36-41.

Attia, U. M., Marson, S., Alcock, J. R., 2009. Micro-injection moulding of polymer microfluidic devices. Microfluidics and Nanofluidics, 7(1), 1-28.

Attia, U. M., Alcock, J. R., 2009. An evaluation of process-parameter and part-geometry effects on the quality of filling in micro-injection moulding. Microsystem technologies, 15(12), 1861-1872.

Berger, G. R., Steffel, C., Friesenbichler, W., 2016. A study on the role of wetting parameters on friction in injection moulding. International Journal of Materials and Product Technology, 52(1-2), 193-211.

Correia, M. S., Miranda, A. S., Oliveira, M. C., Capela, C. A., Pouzada, A. S., 2012. Analysis of friction in the ejection of thermoplastic mouldings. The International Journal of Advanced Manufacturing Technology, 59(9-12), 977-986.

Delaney, K. D., Bissacco, G., Kennedy, D., 2012. A structured review and classification of demolding issues and proven solutions. International Polymer Processing, 27(1), 77-90.

Delaney, K., Kennedy, D., 2010. Demoulding force prediction for micro polymer replication: a review of relevant literature. Dublin Institute of Technology.

Dhanorker, A., Liu, X., Özel, T., 2007. Micromilling process planning and modeling for micromold manufacturing. In ASME 2007 International Manufacturing Science and Engineering Conference (pp. 759-769). American Society of Mechanical Engineers.

Dong, W. P., Sullivan, P. J., Stout, K. J., 1994. Comprehensive study of parameters for characterising three-dimensional surface topography: III: Parameters for characterising amplitude and some functional properties. Wear, 178(1), 29-43.

Ferreira, E. C., Costa, M. F., Laranjeira, C. R., Oliveira, M. J., Pouzada, A. S., 2004. Comparative study, by optical techniques of the interface polymer/steel in replication conditions. In Materials Science Forum (Vol. 455, pp. 467-471). Trans Tech Publications.

Giboz, J., Copponnex, T., Mélé, P., 2007. Microinjection molding of thermoplastic polymers: a review. Journal of Micromechanics and Microengineering, 17(6), R96.

Griffiths, C. A., Dimov, S. S., Brousseau, E. B., Chouquet, C., Gavillet, J., Bigot, S., 2010. Investigation of surface treatment effects in micro-injection-moulding. The International Journal of Advanced Manufacturing Technology, 47(1-4), 99-110.

Griffiths, C. A., Tosello, G., Dimov, S. S., Scholz, S. G., Rees, A., Whiteside, B., 2015. Characterisation of demoulding parameters in micro-injection moulding. Microsystem Technologies, 21(8), 1677-1690.

Heckele, M., Schomburg, W. K., 2003. Review on micro molding of thermoplastic polymers. Journal of Micromechanics and Microengineering, 14(3), R1.

Huo, D., 2013. Micro-cutting: fundamentals and applications. John Wiley & Sons.

ISO13565-2: 1998. Geometric Product Specifications (GPS) - Surface texture: Profile method - Surfaces having stratified functional properties - Part 2: Height characterization using linear material ratio curve.

ISO4287: 1998. Geometrical product specification (GPS) - Surface texture: Profile method - Terms, definitions and surface texture parameters.

Kim, D. E., Suh, N. P., 1991. On microscopic mechanisms of friction and wear. Wear, 149(1), 199-208.

Kim, D. E., Suh, N. P., 1993. Frictional behavior of extremely smooth and hard solids. Wear, 162, 873-879.

Lucchetta, G., Marinello, F., Bariani, P. F., 2011. Aluminum sheet surface roughness correlation with adhesion in polymer metal hybrid overmolding. CIRP Annals-Manufacturing Technology, 60(1), 559-562.

Lucchetta, G., Masato, D., Sorgato, M., Crema, L., Savio, E. 2016. Effects of different mould coatings on polymer filling flow in thin-wall injection moulding. CIRP Annals-Manufacturing Technology, 65(1), 537-540.

Lucchetta, G., Sorgato, M., Carmignato, S., Savio, E., 2014. Investigating the technological limits of micro-injection molding in replicating high aspect ratio micro-structured surfaces. CIRP Annals-Manufacturing Technology, 63(1), 521-524.

Majewski, C., & Hopkinson, N., 2003. Effect of tool finishing on ejection forces for injection moulded parts made using direct metal laser sintered tools. International journal of production research, 41(3), 581-592.

Marson, S., Attia, U. M., Lucchetta, G., Wilson, A., Alcock, J. R., Allen, D. M., 2011. Flatness optimization of micro-injection moulded parts: the case of a PMMA microfluidic component. Journal of Micromechanics and Microengineering, 21(11), 115024.

Masato, D., Sorgato, M., Lucchetta G., 2016. Analysis of the influence of part thickness on the replication of micro-structured surfaces by injection molding. Materials & Design, 95:219-224.

Masuzawa, T., 2000. State of the art of micromachining. CIRP Annals-Manufacturing Technology, 49(2), 473-488.

Menges, G., Michaeli, W., Mohren, P., 2001. How to make injection molds (p. 631). Carl Hanser Verlag GmbH & Co. KG.

Parenti, P., Masato, D., Sorgato, M., Lucchetta, G., Annoni, M., 2016. Surface footprint in molds micromilling and effect on part demoldability in micro injection molding, Journal of Manufacturing Processes, 2017.

Parenti, P., Pagani, L., Annoni, M., Colosimo, B. M., Semeraro, Q., 2016. On the geometrical accuracy of high aspect ratio micromilled pins, Journal of Manufacturing Science and Engineering, under publication.

Pontes, A. J., Pouzada, A. S., 2004. Ejection force in tubular injection moldings. Part I: Effect of processing conditions. Polymer Engineering & Science, 44(5), 891-897.

Pontes, A. J., Pouzada, A. S., 2006. Predicting shrinkage in semi-crystalline injection mouldings–the influence of pressure. In Materials science forum (Vol. 514, pp. 1501-1505). Trans Tech Publications.

Pouzada, A. S., Ferreira, E. C., Pontes, A. J., 2006. Friction properties of moulding thermoplastics. Polymer Testing, 25(8), 1017-1023.

Sasaki, T., Koga, N., Shirai, K., Kobayashi, Y., Toyoshima, A., 2000. An experimental study on ejection forces of injection molding. Precision engineering, 24(3), 270-273.

Schaller, T., Heckele, M., Ruprecht, R., Schubert, K., 1999. Microfabrication of a mold insert made of hardened steel and first molding results. In Proceedings of the ASPE (Vol. 20, pp. 224-227).

Sorgato, M., Masato, D., Lucchetta, G., 2016. Effect of vacuum venting and mold wettability on the replication of micro-structured surfaces. Microsystem Technologies.

Suh, N. P., Mosleh, M., Howard, P. S., 1994. Control of friction. Wear, 175(1), 151-158.

Tao Zhang, M., Bartolo, P., Vasco, J., Silva, B., Galo, C., 2006. Laser micromachining for mould manufacturing: I. The influence of operating parameters. Assembly Automation, 26(3), 227-234.

Wu, S., 1982. Polymer interface and adhesion. M. Dekker.

Yao, D., Kim, B., 2004. Scaling issues in miniaturization of injection molded parts. Journal of Manufacturing Science and Engineering, 126(4), 733-739.

Zhang, H. L., Ong, N. S., Lam, Y. C., 2007. Effects of surface roughness on microinjection molding. Polymer Engineering & Science, 47(12), 2012-2019.

Figure captions

Figure 1: Example of multi-layer chip: 2 functional polymer layers - 2 PDMS sealing membranes.

Figure 2: Micro milling of a lab-on-a-chip mold: 4 arrays of 28 pins - diameter 0.8 mm, height 2 mm.

Figure 3: Design of the study part. All dimensions are expressed in millimeters.

Figure 4: Main micro tooling components: ejector rod and micro-milled pins (diameter: 1 mm).

Figure 5: Main micro tooling components: mold cavity (SEM micrograph, magnification: 35x).

Figure 6: Experimental flow curve for the two polymers at µIM experimental melt temperature (i.e. 240 °C for PS and at 300 °C for COC).

Figure 7: Mold assembly - details of the moving half.

Figure 8: Stabilization behavior of the dry ejection force over cycles for Sample 1.

Figure 9: Response variables for the statistical analysis of the experimental data.

Figure 10: Example of demolding force in-line acquisitions of DoE repetitions - std. dev. F_{peak}: 0.38 N, F_{area}: 0.75 N·s.

Figure 11: SEM micrographs of the micro-milled mold inserts at different magnifications. Insert 1 at (a) 200x and (d) 500x; Insert 2 at (b) 200x and (e) 500x; Insert 3 at (c) 200x and (f) 500x.

Figure 12: 3D and 2D views of the three mold insert topographies.

Figure 13: Histograms of roughness parameters for (a) ISO 4287 and (b) ISO 13565-2.

Figure 14: Main effect plots for the demolding peak force F_{peak} (screening plan).

Figure 15: Main effect plots for the demolding work F_{area} (screening plan).

Figure 16: Effect of the micro milling strategy on the demolding force curves - max. standard deviation: 0.5 N.

Figure 17: Interaction plot for the optimization plan. (a) demolding force peak; (b) demolding force area.

Figure 18: Roughness amplitude parameters evaluated on the plastic parts.

Figure 19: SEM micrographs of the molded parts topographies - magnification: 2000x.

Table captions

Table 1: Micro milling strategies for the finishing operations of cores side.

Table 2: Main properties of the investigated polymers.

Table 3: Process parameters settings for the screening DoE plan.

Table 4: Process parameters settings for the optimization plan.

Table 5: Average values and standard deviations of profile roughness parameters evaluated according to ISO 4287 and ISO 13565-2.

Table 6: Anova table for the screening experiments designed in Table 3.

Table 7: Anova table for the optimization experiments designed in Table 4.

Table 8: Experimental results of the optimization plan.

Table 9: Molded parts roughness (optimization plan).